Substitutional Isomerism for Trimetallic Clusters Having Icosahedral Ligand Arrangements. The Crystal Structures of $(\mu\text{-H})Ru_3[\mu\text{-CN}(CH_3)_2](CO)_9(C_5H_5N)$ and $(\mu\text{-H})Ru_3[\mu\text{-CN}(CH_2C_6H_5)_2](CO)_9(PPh_3)$

Melvyn Rowen Churchill,* James C. Fettinger, and Jerome B. Keister*

Department of Chemistry, State University of New York at Buffalo, Buffalo, New York 14214

Received March 7, 1985

The crystal structures of two structural isomers $(\mu\text{-H})Ru_3(\mu\text{-CNR}_2)(CO)_9L$ (R = Me, L = py; R = Bz, L = PPh_3) have been determined.[1] The complex $(\mu\text{-H})Ru_3(\mu\text{-CNMe}_2)(CO)_9(py)$ crystallizes in the centrosymmetric triclinic space group $P\bar{1}$ (No. 2) with a = 8.0650 (11) Å, b = 9.2237 (13) Å, c = 16.9384 (29) Å, α = 94.274 (19)°, β = 100.837 (13)°, γ = 106.725 (13)°, V = 1174.1 (3) Å^3, and Z = 2. Diffraction data (Mo Kα, 2θ = 5–50°) were collected on a Syntex $P2_1$ diffractometer, and the structure was refined to R_F = 4.1% for all 3925 data (R_F = 2.4% for those 2649 reflections with $|F_o| > 6\sigma(|F_o|)$). The dibridged Ru–Ru bond is 2.802 (1) Å in length, and the nonbridged Ru–Ru distances are 2.855 (1) and 2.844 (1) Å. The py ligand occupies a "semiaxial" site on one of the dibridged ruthenium atoms (Ru(1)–N(1) = 2.250 (5) Å) and causes some asymmetry in the trans μ-CNMe ligand. The species $(\mu\text{-H})Ru_3(\mu\text{-CNBz}_2)(CO)_9(PPh_3)$ crystallizes in the noncentrosymmetric orthorhombic space group $Pna2_1$ (No. 33) with a = 17.879 (5) Å, b = 13.735 (4) Å, c = 17.122 (5) Å, V = 4204 (2) Å^3, and Z = 4. Diffraction data (Mo Kα, 2θ = 4.5–45°) were collected, and the structure was refined to R_F = 5.9% for all 5311 data (R_F = 4.2% for those 4128 reflections with $|F_o| > 6\sigma(|F_o|)$. The dibridged Ru–Ru bond is 2.792 (1) Å in length, and the bulky PPh_3 ligand occupies an equatorial site on the nonbridged ruthenium atom (Ru(2)–P = 2.384 (2) Å). The Ru–Ru bond cis to the PPh_3 ligand (Ru(2)–Ru(3) = 2.885 (1) Å) is lengthened relative to that trans to the PPh_3 ligand (Ru(1)–Ru(2) = 2.844 (1) Å). These structures bring the number of known isomers of $(\mu\text{-H})M_3(\mu\text{-CX})(CO)_9L$ to four. Steric effects upon the thermodynamic stabilities of these isomers are examined.

Introduction

Systematic investigations of the structures and reactivities of methylidynetriruthenium and -osmium clusters $HM_3(CX)(CO)_{10}$ and $H_3M_3(CX)(CO)_9$ allow the assessment of the variation in cluster properties as a function of the methylidyne substituent, the metal, and the other cluster ligands.[2-6] Recent studies in our laboratories have focused upon the mechanism of ligand substitution on $(\mu\text{-H})Ru(\mu\text{-CX})(CO)_{10}$ (X = OMe, NR_2) by group 15[36] donor ligands L to form $(\mu\text{-H})Ru_3(\mu\text{-CX})(CO)_9L$.[7] Spectroscopic characterizations of these products indicated the existence of at least two substitutional isomers. One of these was shown by ^{13}C NMR spectroscopy to be substituted on a bridged metal atom and in an equatorial coordination site, but the identities of the other(s) could not be determined by spectroscopic methods. Since the identities of these isomers were vital to the determination of the mechanism of ligand substitution and since we have previously established that the bonding mode of the methylidyne ligand may change upon ligand substitution,[2a] we have determined the crystal structures of $(\mu\text{-H})Ru_3(\mu\text{-CNMe}_2)(CO)_9(py)$ and $(\mu\text{-H})Ru_3(\mu\text{-CNBz}_2)(CO)_9(PPh_3)$.[1] These structures, in combination with those already reported, bring to four the number of substituted isomers for clusters of the formula $M_3(\mu\text{-X})(\mu\text{-Y})(CO)_9L$, for which the ligand shell may be described as an icosahedron. These results allow some generalizations to be made concerning the steric and electronic factors which determine the stabilities of these four isomeric forms.

Experimental Section

The syntheses of $(\mu\text{-H})Ru_3(\mu\text{-CNMe}_2)(CO)_9(py)$ and $(\mu\text{-H})Ru_3(\mu\text{-CNBz}_2)(CO)_9(PPh_3)$ were accomplished according to procedures published previously.[7] Recrystallization of $(\mu\text{-H})Ru_3(\mu\text{-CNMe}_2)(CO)_9(py)$ from methanol containing excess pyridine provided suitable crystals. Crystals of $(\mu\text{-H})Ru_3(\mu\text{-CNBz}_2)(CO)_9(PPh_3)$ were obtained from an ethanol–2-propanol solution by slow evaporation.

Collection of X-ray Diffraction Data for $(\mu\text{-H})Ru_3(\mu\text{-CNMe}_2)(CO)_9(py)$. A series of crystals were sealed into thin-walled glass capillary tubes. That finally selected for the X-ray diffraction study was a well-formed parallelepiped with approximate orthogonal dimensions of 0.2 mm × 0.2 mm × 0.3 mm; it was mounted along its extended direction in a eucentric goniometer and was aligned and accurately centered on our Syntex $P2_1$ automated four-circle diffractometer. Set-up procedures (i.e., determination of unit-cell dimensions and the crystal's orientation matrix) and data collection were carried out as has been described previously;[8] details appear in Table I. The final cell parameters are derived by a least-squares analysis of the setting angles (2θ, ω, χ) determined from the automated centering of 25 reflections (well dispersed in reciprocal space) with 2θ = 20–30°. [We chose reflections in this angular range so as to ensure that all peaks were the *unresolved* Mo K$\bar{a}$ reflections.] The diffraction pattern had only Friedel symmetry (C_i, $\bar{1}$) with no systematic absences. The crystals therefore belong to the triclinic system. Possible space groups are the noncentrosymmetric triclinic space group $P1$ (C_1^1;

(1) Abbreviations: Me = CH_3; py = C_5H_5N (pyridine); Bz = $CH_2C_6H_5$ (benzyl); Ph = C_6H_5.

(2) (a) Churchill, M. R.; Beanan, L. R.; Wasserman, H. J.; Bueno, C.; Abdul Rahman, Z.; Keister, J. B. *Organometallics* **1983**, *2*, 1179. (b) Churchill, M. R.; DeBoer, B. G.; Rotella, F. J. *Inorg. Chem.* **1976**, *15*, 1843.

(3) (a) Keister, J. B.; Payne, M. W.; Muscatella, M. J. *Organometallics* **1983**, *2*, 219. (b) Keister, J. B.; Horling, T. L. *Inorg. Chem.* **1980**, *19*, 2304. (c) Abdul Rahman, Z.; Beanan, L. R.; Bavaro, L. M.; Modi, S. P.; Keister, J. B.; Churchill, M. R. *J. Organomet. Chem.* **1984**, *263*, 75. (d) Bavaro L. M.; Montangero, P.; Keister, J. B. *J. Am. Chem. Soc.* **1983**, *105*, 4977. (e) Sherwood, D. E., Jr.; Hall, M. B. *Organometallics* **1982**, *1*, 1519. (f) Holmgren, J. S.; Shapley, J. R. *Organometallics* **1984**, *3*, 1322. (g) Shapley, J. R.; Cree- Uchiyama, M. E.; St. George, G. M.; Churchill, M. R.; Bueno, C. *J. Am. Chem. Soc.* **1983**, *105*, 140.

(4) Johnson, B. F. G.; Lewis, J.; Orpen, A. G.; Raithby, P. R.; Suss, G. *J. Organomet. Chem.* **1979**, *173*, 187.

(5) Yeh, W.-Y.; Shapley, J. R.; Li, Y.-J.; Churchill, M. R. *Organometallics* **1985**, *4*, 767.

(6) (a) Beanan, L. R.; Abdul Rahman, Z.; Keister, J. B. *Organometallics* **1983**, *2*, 1062. (b) Beanan, L. R.; Keister, J. B. *Organometallics*, in press.

(7) Dalton, D. M.; Barnett, D. J.; Duggan, T. P.; Keister, J. B.; Malik, P. T.; Modi, S. P.; Shaffer, M. R.; Smesko, S. A. *Organometallics*, preceding paper in this issue.

(8) Churchill, M. R.; Lashewycz, R. A.; Rotella, F. J. *Inorg. Chem.* **1977**, *16*, 265.

0276-7333/85/2304-1867$01.50/0

Table I. Experimental Data for the X-ray Diffraction Studies of $(\mu\text{-H})Ru_3(\mu\text{-CNMe}_2)(CO)_9(py)$ and $(\mu\text{-H})Ru_3(\mu\text{-CNBz}_2)(CO)_9(PPh_3)$

	$(\mu\text{-H})Ru_3(\mu\text{-CNMe}_2)(CO)_9(py)$	$(\mu\text{-H})Ru_3(\mu\text{-CNBz}_2)(CO)_9(PPh_3)$
	(A) Unit Cell Parameters at 24 °C (297 K)	
cryst system	triclinic	orthorhombic
space group	$P\bar{1}$ (no. 2)	$Pna2_1$ (no. 33)
a, Å	8.0650 (11)	17.879 (5)
b, Å	9.2237 (13)	13.735 (4)
c, Å	16.9384 (29)	17.122 (5)
α, deg	94.274 (19)	(90)
β, deg	100.837 (13)	(90)
γ, deg	106.725 (13)	(90)
V, Å^3	1174.1 (3)	4204 (2)
formula	$C_{17}H_{12}N_2O_9Ru_3$	$C_{42}H_{30}NO_9PRu_3$
mol wt	691.50	1026.89
Z	2	4
D(calcd), g/cm^3	1.96	1.62
μ(Mo Kα), cm^{-1}	19.1	11.3
	(B) Collection of X-ray Diffraction Data	
diffractometer	Syntex $P2_1$	[a]
radiatn	Mo K$\bar{\alpha}$ ($\bar{\lambda}$ = 0.710730 Å)	[a]
monochromator	highly oriented (pyrolytic) graphite, 2θ(m) = 12.160° for 002 reflection; equatorial mode; assumed 50% perfect/50% ideally mosaic for polarization corrections	[a]
reflctns collected	$+h, \pm k, \pm l$ for 2θ = 5.0–50.0°; 4479 reflctns merged to 4160 unique data (3925 with $I > 0$ were retained)	$+h, +k, \pm l$ for 2θ = 4.5–45.0°; 6223 reflctns merged to 5311 *point*-group independent data with $I > 0$
scan type	coupled θ(crystal)–2θ(counter)	[a]
scan speed	4.0 deg/min	[a]
scan width	$[2\theta(K\alpha_1) - 0.9] \rightarrow [2\theta(K\alpha_2) + 0.9]$ deg	[a]
bkgds	stationary crystal and stationary counter; measured at each end of the 2θ scan (each for one-fourth total scan time)	[a]
stds	3 approximately orthogonal reflctns remeasd after each batch of 97 reflctns; no decay or significant fluctuatns were obsd	[a]

[a] Conditions as described in previous column

no. 1) or the centrosymmetric triclinic space group $P\bar{1}$ (C_i^1; no. 2). The latter centrosymmetric possibility was indicated by the number of molecules per unit cell ($Z = 2$) and by intensity statistics; it was confirmed by the successful solution of the structure in this higher space group.

All data were corrected for absorption and for Lorentz and polarization effects and were converted to unscaled $|F_o|$ values; any datum with I(net) < 0 was omitted.

Refinement of the Structure of $(\mu\text{-H})Ru_3(\mu\text{-CNMe}_2)(CO)_9(py)$. The structure solution and refinement was carried out by using the SHELX76 program set of G. M. Sheldrick on the SUNY—Buffalo CDC Cyber 173 computer. The calculated structure factors were based upon the analytical form of the neutral atoms' scattering factors and were corrected for both the real ($\Delta f'$) and imaginary ($i\Delta f''$) components of anomalous dispersion.[9] The function minimized in least-squares procedures was $\sum w(|F_o| - |F_c|)^2$.

The positions of the three ruthenium atoms were determined by direct methods using symbolic addition. All remaining nonhydrogen atoms were located from a subsequent difference Fourier synthesis. All hydrogen atoms were located from a second difference Fourier synthesis, following refinement of isotropic thermal parameters and positional parameters of all non-hydrogen atoms. The structure was refined to convergence using the "block-cascade" technique. All positional parameters, anisotropic thermal parameters for non-hydrogen atoms, and isotropic thermal parameters for all hydrogen atoms were refined. Final discrepancy indices were[10] R_F = 4.1% and R_{wF} = 4.2% for 328 parameters refined against all 3925 unique non-negative data (R_F = 2.9% and R_{wF} = 3.4% for those 3188 reflections with $|F_o| > 3\sigma(|F_o|)$; R_F = 2.4% and R_{wF} = 2.8% for those 2649 reflections with $|F_o| > 6\sigma(|F_o|)$).

A final difference Fourier map showed no remaining significant features; the structure is thus both correct and complete. Final positional parameters are collected in Table II; anisotropic thermal parameters have been deposited.[11]

Collection of X-ray Diffraction Data for $(\mu\text{-H})Ru_3(\mu\text{-CNBz}_2)(CO)_9(PPh_3)$. A crystal of approximate orthogonal dimensions 0.15 × 0.2 × 0.3 mm^3 was sealed into a thin-walled glass capillary and aligned on our Syntex $P2_1$ diffractometer as described above; details of unit cell dimensions and data collection appear in Table I. The final cell parameters are based upon the setting angles of 25 reflections with 2θ = 20–24°. The crystal showed D_{2h} (mmm) diffraction symmetry and therefore belongs to the orthorhombic system. The systematic absences $0kl$ for $k + l = 2n + 1$ and $h0l$ for $h = 2n + 1$ ($00l$ for $l = 2n + 1$) are consistent with the noncentrosymmetric space group $Pna2_1$ (C_{2v}^9; no. 33) or with the centrosymmetric space group $Pnam$, a nonstandard setting of $Pnma$ (D_{2h}^{16}; no. 62). Intensity statistics favored the acentric case; this was confirmed by the successful solution

(9) "International Tables for X-Ray Crystallography"; Kynoch Press: Birmingham, England, 1974; Vol. 4, pp 99–101, 149–150.

(10) $R_F(\%)$ $100\sum||F_o| - |F_c||/\sum|F_o|$; $R_{wF}(\%) = 100[\sum w(|F_o| - |F_c|)^2/\sum w|F_o|^2]^{1/2}$.

(11) See final paragraph at the end of this paper concerning "Supplementary Material Available".

Table II. Final Positional Parameters for $(\mu\text{-}H)Ru_3(\mu\text{-}CNMe_2)(CO)_9(py)$

atom	x	y	z	U, Å²
Ru(1)	0.19533 (5)	0.09375 (4)	0.19003 (3)	
Ru(2)	0.39595 (5)	0.19771 (4)	0.34872 (2)	
Ru(3)	0.18328 (6)	0.36932 (5)	0.27410 (3)	
C(11)	−0.0374 (8)	0.0652 (6)	0.1363 (4)	
O(11)	−0.1831 (7)	0.0482 (6)	0.1049 (4)	
C(12)	0.2039 (8)	−0.0993 (7)	0.1504 (4)	
O(12)	0.2048 (8)	−0.2195 (6)	0.1294 (4)	
C(21)	0.3411 (8)	0.2588 (7)	0.4481 (4)	
O(21)	0.3096 (7)	0.2978 (6)	0.5077 (3)	
C(22)	0.6187 (7)	0.3680 (6)	0.3649 (3)	
O(22)	0.7487 (6)	0.4620 (5)	0.3739 (3)	
C(23)	0.5081 (7)	0.0537 (7)	0.3870 (4)	
O(23)	0.5730 (7)	−0.0339 (6)	0.4099 (3)	
C(31)	0.0281 (9)	0.4214 (7)	0.1902 (6)	
O(31)	−0.0673 (8)	0.4516 (7)	0.1397 (5)	
C(32)	−0.0088 (9)	0.2454 (8)	0.3169 (6)	
O(32)	−0.1224 (8)	0.1777 (7)	0.3420 (6)	
C(33)	0.2439 (9)	0.5391 (8)	0.3591 (5)	
O(33)	0.2759 (9)	0.6377 (7)	0.4093 (5)	
C(34)	0.3918 (8)	0.4504 (7)	0.2308 (4)	
O(34)	0.5134 (6)	0.5034 (5)	0.2051 (3)	
N(1)	0.3115 (6)	0.1990 (5)	0.0892 (3)	
C(1)	0.2270 (9)	0.2655 (7)	0.0341 (4)	
C(2)	0.2980 (13)	0.3190 (8)	−0.0313 (4)	
C(3)	0.4543 (11)	0.3027 (8)	−0.0412 (4)	
C(4)	0.5392 (9)	0.2348 (8)	0.0133 (4)	
C(5)	0.4671 (8)	0.1832 (7)	0.0777 (3)	
C(6)	0.1604 (6)	0.0337 (5)	0.2968 (3)	
N(2)	0.0457 (6)	−0.0729 (5)	0.3224 (3)	
C(7)	0.0576 (13)	−0.0938 (9)	0.4078 (5)	
C(8)	−0.1166 (10)	−0.1813 (9)	0.2684 (6)	
H	0.420 (9)	0.161 (8)	0.247 (4)	0.10 (2)
H(1)	0.118 (7)	0.277 (6)	0.043 (3)	0.04 (1)
H(2)	0.232 (11)	0.353 (10)	−0.062 (5)	0.12 (3)
H(3)	0.512 (7)	0.332 (6)	−0.085 (4)	0.07 (2)
H(4)	0.661 (11)	0.223 (10)	0.013 (5)	0.14 (3)
H(5)	0.544 (7)	0.140 (7)	0.129 (4)	0.08 (2)
H(71)	−0.042 (12)	−0.080 (10)	0.418 (5)	0.13 (3)
H(72)	0.026 (15)	−0.192 (14)	0.417 (7)	0.19 (5)
H(73)	0.178 (12)	−0.042 (10)	0.444 (5)	0.11 (3)
H(81)	−0.123 (10)	−0.187 (9)	0.214 (5)	0.12 (3)
H(82)	−0.137 (11)	−0.272 (10)	0.284 (5)	0.12 (3)
H(83)	−0.256 (12)	−0.154 (11)	0.269 (6)	0.15 (3)

of the structure in the noncentrosymmetric space group. Data were reduced to unscaled $|F_o|$ values as described above.

Refinement of the Structure of $(\mu\text{-}H)Ru_3(\mu\text{-}CNBz_2)(CO)_9(PPh_3)$. The structure solution was carried out by using the SHELX76 program set (vide infra). Once all non-hydrogen atoms had been located, full-matrix least-squares refinement was continued in-house with the SUNY—Buffalo modified version of the Syntex XTL interrogative crystallographic program package. Each of the possible enantiomers was tested (by changing all atomic coordinates from x, y, z to $1-x, 1-y, 1-z$); that with the lowest discrepancy indices was adjudged correct. Positional parameters for all non-hydrogen atoms (save for the origin-defining z coordinate of Ru(3)) were refined, as were those for the bridging hydride ligand. Anisotropic thermal parameters were refined for atoms in the $Ru_3(\mu\text{-}CNC_2)(CO)_9(P)$ portion of the molecule; carbon atoms of all phenyl groups were refined isotropically and all hydrogen atoms (except for the bridging hydride ligand) were placed in calculated positions based upon $d(C\text{–}H) = 0.95$ Å and the appropriate trigonal or tetrahedral disposition about the attached carbon atom.[12] Refinement for the correct enantiomer converged with $R_F = 5.9\%$ and $R_{wF} = 4.8\%$ for all 5311 *point-group* independent data ($R_F = 5.1\%$ and $R_{wF} = 4.7\%$ for those 4806 reflections with $|F_o| > 3\sigma(|F_o|)$; $R_F = 4.2\%$ and $R_{wF} = 4.4\%$ for those 4128 reflections with $|F_o| > 6\sigma(|F_o|)$).

A final difference Fourier synthesis revealed no unexpected features; the structure is thus correct and complete. Final positional parameters are collected in Table III; anisotropic thermal parameters have been deposited.[11]

(12) Churchill, M. R. *Inorg. Chem.* **1973**, *12*, 1213.

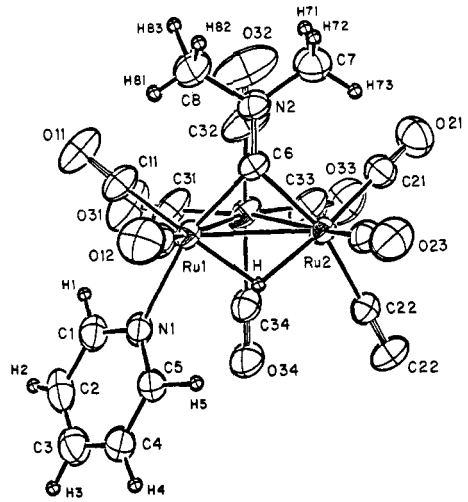

Figure 1. Labeling of atoms in the $(\mu\text{-}H)Ru_3(\mu\text{-}CNMe_2)(CO)_9(py)$ molecule (ORTEP-II diagram, with all hydrogen atoms shown as reduced spheres in their refined positions).

Results

Description of the Molecular Structure of $(\mu\text{-}H)Ru_3(\mu\text{-}CNMe_2)(CO)_9(py)$. This complex crystallizes as an ordered racemic mixture of two enantiomeric forms in discrete monomeric units separated by normal van der Waals' distances. The atomic numbering scheme is given by Figure 1; a stereoscopic view of the molecule appears as Figure 2. Interatomic distances and angles are listed in Tables IV and V.

The derived molecular structure bears a very close resemblance to that of the parent complex $(\mu\text{-}H)Ru_3(CNMe_2)(CO)_{10}$, previously reported by Churchill, DeBoer, and Rotella.[2] Thus the dibridged Ru(1)–Ru(2) distance of 2.802 (1) Å is slightly shorter than the nonbridged ruthenium–ruthenium distances Ru(1)–Ru(3) = 2.855 (1) Å and Ru(2)–Ru(3) = 2.844 (1) Å (cf. Ru–Ru(bridged) = 2.7997 (5)–2.8016 (6) Å and Ru–Ru(nonbridged) = 2.8216 (6)–2.8336 (6) Å in the parent complex). The individual Ru–CO distances range from Ru(1)–C(11) = 1.860 (6) Å through Ru(2)–C(22) = 1.974 (5) Å. The longest such bond length (Ru(2)–C(22)) is for the sole carbonyl ligand trans to the μ-C=NMe_2 ligand; this suggests that the μ-C=NMe_2 ligand competes effectively with the terminal carbonyl ligand for π-electron density from Ru(2). The pyridine ligand (a good σ-donor, but a poor π-acceptor) occupies a "semiaxial" site on Ru(1), adjacent to the bridging hydride ligand and trans to the μ-C=NMe_2. The Ru(1)–N(1) bond length is 2.250 (5) Å. The marked difference between the two ligands trans to the μ-C=NMe_2 group causes a significant asymmetry in its bonding to the metal atoms. The Ru(1)–C(6) distance of 1.977 (6) Å (trans to the σ-donating py ligand) is some 0.07 Å shorter than the Ru(2)–C(6) distance of 2.047 (4) Å (trans to the π-acceptor ligand C(22)–O(22)). The C=NMe_2 ligand is clearly present in the 1,2-dipolar ylide form (see I) as is evidenced by the N(2)–C(6) distance of 1.304 (7) Å being some ~0.16–0.18 Å shorter than the bonds N(2)–C(7) = 1.463 (10) Å and N(2)–C(8) = 1.486 (8) Å.

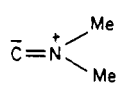

I

The μ-hydride ligand was located with reasonable precision and is symmetrically located with Ru(1)–H = 1.79 (6) Å, Ru(2)–H = 1.79 (7) Å, and ∠Ru(1)–H–Ru(2) = 103

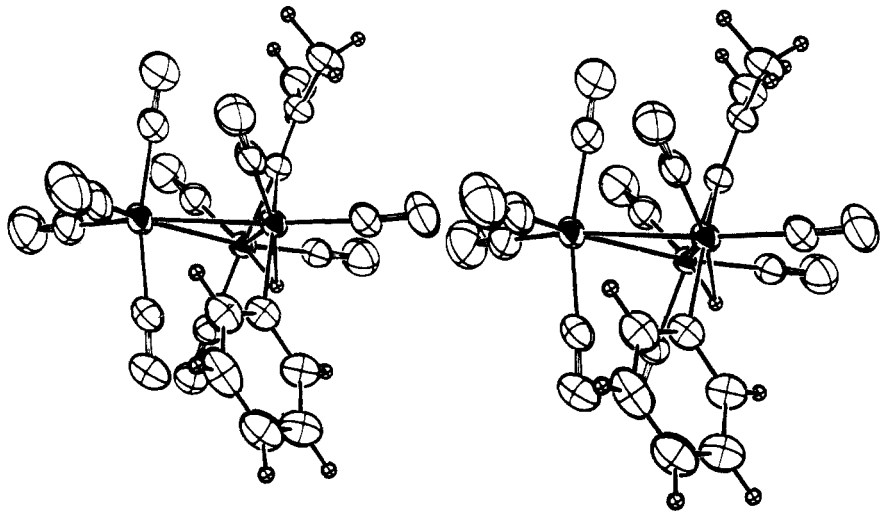

Figure 2. Stereoscopic view of the $(\mu\text{-H})Ru_3(\mu\text{-CNMe}_2)(CO)_9(py)$ molecule.

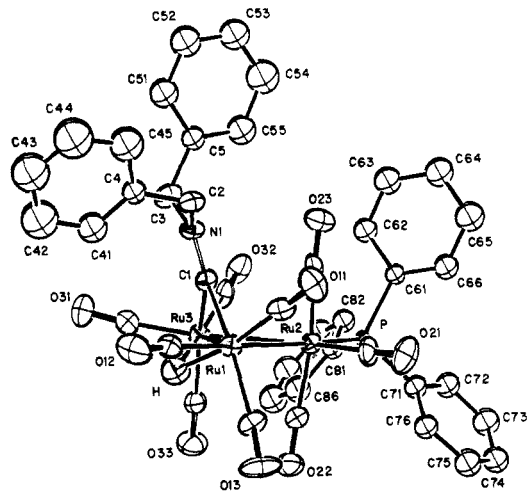

Figure 3. Numbering of atoms in the $(\mu\text{-H})Ru_3(\mu\text{-CNBz}_2)(CO)_9(PPh_3)$ molecule (ORTEP-II diagram, with all hydrogen atoms omitted other than the μ-hydride ligand).

(4)°. The μ-C=NMe ligand is associated with an acute Ru(1)–C(6)–Ru(2) angle of 88.2 (2)°.

Description of the Molecular Geometry of $(\mu\text{-H})Ru_3(\mu\text{-CNBz}_2)(CO)_9(PPh_3)$. This molecule, like the previous one, is inherently asymmetric. It, too, crystallizes as an ordered racemic mixture of the two enantiomeric forms with no abnormally short contacts between the molecular units. The molecular geometry is illustrated in Figure 3; a stereoscopic view of the molecule is afforded by Figure 4. Interatomic distances and angles are collected in Tables VI and VII.

The dibridged Ru(1)–Ru(3) bond length of 2.792 (1) Å is, again, shorter than the nonbridged ruthenium–ruthenium distances Ru(1)–Ru(2) = 2.844 (1) Å and Ru(2)–Ru(3) = 2.885 (1) Å. Individual Ru–CO distances range from Ru(3)–C(31) = 1.852 (12) Å through Ru(1)–C(13) = 1.984 (11) Å; two of the longest such distances are trans to the μ-C=NBz$_2$ ligand (i.e., Ru(1)–C(13) = 1.984 (11) Å and Ru(3)–C(33) = 1.931 (12) Å). The two Ru–C(1) distances are approximately equivalent with Ru(1)–C(1) = 2.052 (10) Å, Ru(3)–C(1) = 2.041 (11) Å, and ∠Ru(1)–C(1)–Ru(3) = 86.0 (4)°. The μ-C=NBz$_2$ ligand clearly contains discrete double and single bonds with N(1)–C(1) = 1.288 (14) Å vis à vis N(1)–C(2) = 1.482 (13) Å and N(1)–C(3) = 1.505 (13) Å. The μ-C=NBz$_2$ ligand appears to block any possible attack of bulky ligands on atoms Ru(1) and Ru(3). The PPh_3 ligand thus occupies an equatorial site on the nonbridged atom Ru(2), with Ru(2)–P = 2.384 (2) Å. This ligand appears to cause few steric problems at Ru(2)—the P–Ru–CO angles are all close to equivalent, with values ranging from P–Ru(2)–C(23) = 93.1 (4)° through P–Ru(2)–C(21) = 96.1 (4)° while cis OC–Ru(2)–CO angles are 89.1 (5)° and 94.6 (5)°. However, the equatorial Ru(3)–Ru(2)–P angle of 111.67 (7)° is some 17.7° greater than the equivalent equatorial angle Ru(1)–Ru(2)–C(21) = 94.0 (4)°. It also seems probable that the PPh_3 ligand is primarily responsible for the Ru(2)–

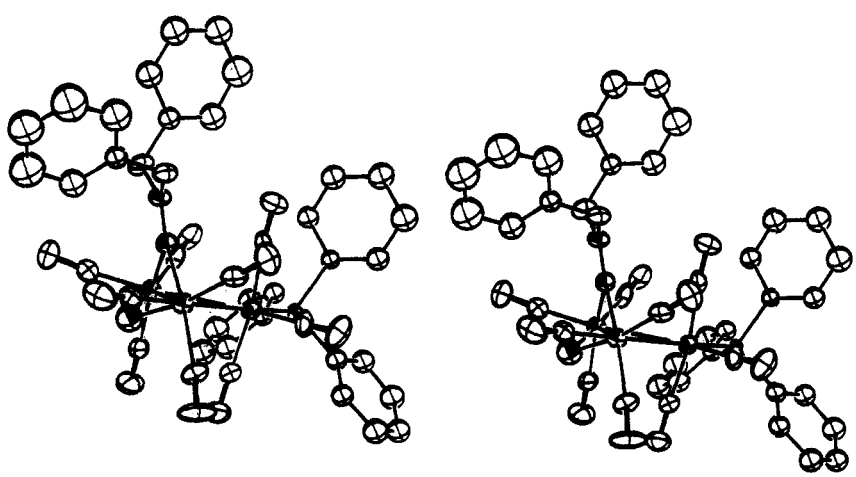

Figure 4. Stereoscopic view of the $(\mu\text{-H})Ru_3(\mu\text{-CNBz}_2)(CO)_9(PPh_3)$ molecule.

Table III. Final Positional Parameters for (μ-H)Ru_3(μ-$CNBz_2$)$(CO)_9(PPh_3)$

atom	x	y	z	B, Å^2	atom	x	y	z	B, Å^2
Ru(1)	−0.03459 (4)	0.21752 (6)	0.95136 (7)		C(65)	0.16886 (81)	0.3944 (10)	0.57180 (83)	6.57 (34)
Ru(2)	0.04178 (4)	0.35841 (6)	0.85936 (8)		C(66)	0.13968 (61)	0.44038 (91)	0.63693 (69)	4.46 (26)
Ru(3)	0.10669 (4)	0.27936 (6)	1.00000 (0)		C(71)	0.07962 (60)	0.58671 (79)	0.76384 (64)	3.70 (23)
H	−0.0017 (60)	0.2317 (80)	1.0411 (60)	5.9 (31)	C(72)	0.12286 (69)	0.65571 (93)	0.72437 (73)	5.06 (27)
P	0.12313 (12)	0.47285 (17)	0.79822 (14)		C(73)	0.09181 (72)	0.7429 (10)	0.70001 (76)	5.93 (30)
C(1)	0.07023 (52)	0.15764 (80)	0.94322 (64)		C(74)	0.01948 (68)	0.76109 (94)	0.71225 (76)	5.14 (28)
N(1)	0.09810 (43)	0.07433 (62)	0.92469 (48)		C(75)	−0.02595 (70)	0.6955 (10)	0.74764 (76)	5.55 (30)
C(2)	0.05116 (55)	−0.00914 (79)	0.90007 (63)		C(76)	0.00575 (64)	0.60913 (83)	0.77515 (65)	4.30 (25)
C(4)	0.04533 (58)	−0.08852 (78)	0.96024 (66)	3.78 (22)	C(81)	0.20335 (51)	0.52631 (72)	0.85150 (65)	3.40 (21)
C(41)	0.04502 (75)	−0.0690 (10)	1.03744 (80)	5.68 (30)	C(82)	0.27424 (62)	0.54313 (82)	0.82111 (65)	4.29 (25)
C(42)	0.0348 (10)	−0.1433 (14)	1.0921 (11)	9.39 (48)	C(83)	0.33063 (69)	0.58570 (93)	0.86708 (82)	5.57 (28)
C(43)	0.0263 (10)	−0.2363 (15)	1.0661 (11)	9.81 (51)	C(84)	0.31410 (86)	0.6114 (11)	0.9401 (10)	6.95 (35)
C(44)	0.0240 (10)	−0.2534 (14)	0.9898 (13)	10.43 (51)	C(85)	0.24846 (80)	0.5960 (10)	0.97340 (81)	6.40 (33)
C(45)	0.03601 (85)	−0.1827 (11)	0.93357 (85)	6.97 (35)	C(86)	0.19114 (73)	0.55545 (93)	0.92707 (72)	5.41 (29)
C(3)	0.17901 (57)	0.04880 (86)	0.93777 (75)		H(2A)	0.0721	−0.0361	0.8539	6.0
C(5)	0.21244 (54)	−0.00346 (78)	0.86676 (73)	3.93 (22)	H(2B)	0.0022	0.0142	0.8892	6.0
C(51)	0.22355 (67)	−0.10370 (91)	0.86965 (83)	5.49 (29)	H(3A)	0.1827	0.0073	0.9820	6.0
C(52)	0.25178 (75)	−0.1522 (10)	0.80547 (87)	6.43 (32)	H(3B)	0.2064	0.1069	0.9470	6.0
C(53)	0.26840 (82)	−0.1037 (11)	0.74195 (87)	6.80 (36)	H(41)	0.0518	−0.0039	1.0548	6.0
C(54)	0.26222 (90)	−0.0067 (12)	0.7376 (10)	8.42 (42)	H(42)	0.0338	−0.1292	1.1463	6.0
C(55)	0.23257 (73)	0.0460 (10)	0.80175 (82)	5.94 (31)	H(43)	0.0220	−0.2885	1.1022	6.0
C(11)	−0.07501 (55)	0.17033 (75)	0.85832 (83)		H(44)	0.0135	−0.3177	0.9728	6.0
O(11)	−0.09868 (44)	0.13989 (67)	0.79986 (50)		H(45)	0.0377	−0.1980	0.8795	6.0
O(12)	−0.07990 (62)	0.12037 (86)	1.01846 (66)		H(51)	0.2116	−0.1387	0.9158	6.0
C(12)	−0.10758 (56)	0.06779 (69)	1.05808 (58)		H(52)	0.2591	−0.2206	0.8074	6.0
C(13)	−0.11516 (58)	0.31281 (81)	0.97395 (68)		H(53)	0.2854	−0.1385	0.6974	6.0
O(13)	−0.15854 (43)	0.36368 (65)	0.99163 (62)		H(54)	0.2776	0.0265	0.6917	6.0
C(21)	−0.03595 (68)	0.37037 (88)	0.78723 (65)		H(55)	0.2269	0.1147	0.7991	6.0
O(21)	−0.08377 (50)	0.37347 (73)	0.74134 (58)		H(62)	0.2440	0.3406	0.7695	6.0
C(22)	0.00167 (57)	0.44959 (82)	0.92941 (67)		H(63)	0.2978	0.2662	0.6609	6.0
O(22)	−0.02258 (44)	0.50823 (64)	0.97216 (48)		H(64)	0.2527	0.2986	0.5363	6.0
C(23)	0.08016 (60)	0.25200 (95)	0.80039 (61)		H(65)	0.1481	0.4062	0.5215	6.0
O(23)	0.09837 (47)	0.18750 (65)	0.76057 (51)		H(66)	0.1002	0.4860	0.6305	6.0
C(31)	0.14288 (61)	0.20858 (89)	1.08391 (68)		H(72)	0.1741	0.6426	0.7141	6.0
O(31)	0.16861 (54)	0.16041 (73)	1.13321 (54)		H(73)	0.1221	0.7899	0.6744	6.0
C(32)	0.19675 (57)	0.30024 (80)	0.94598 (70)		H(74)	−0.0007	0.8216	0.6957	6.0
O(32)	0.25326 (47)	0.31301 (68)	0.91557 (54)		H(75)	−0.0779	0.7080	0.7535	6.0
C(33)	0.10525 (64)	0.40039 (89)	1.05735 (68)		H(76)	−0.0249	0.5643	0.8026	6.0
O(33)	0.10178 (52)	0.47053 (70)	1.09434 (53)		H(82)	0.2847	0.5256	0.7685	6.0
C(61)	0.16638 (53)	0.42157 (71)	0.71033 (57)	3.03 (20)	H(83)	0.3793	0.5959	0.8465	6.0
C(62)	0.22553 (63)	0.35506 (89)	0.71887 (72)	4.43 (25)	H(84)	0.3518	0.6426	0.9700	6.0
C(63)	0.25729 (72)	0.31015 (94)	0.65419 (78)	5.53 (30)	H(85)	0.2401	0.6116	1.0267	6.0
C(64)	0.23066 (74)	0.3287 (10)	0.58069 (87)	6.23 (33)	H(86)	0.1426	0.5481	0.9488	6.0

Table IV. Interatomic Distances (Å), with Esd's, for (μ-H)Ru_3(μ-$CNMe_2$)$(CO)_9$(py)

(A) Ru–Ru and Ru–(Bridging Ligand) Distances

Ru(1)–Ru(2)	2.802 (1)	Ru(1)–C(6)	1.977 (6)
Ru(1)–Ru(3)	2.855 (1)	Ru(2)–C(6)	2.047 (4)
Ru(2)–Ru(3)	2.844 (1)	Ru(1)–H	1.79 (6)
		Ru(2)–H	1.79 (7)

(B) Ru–CO, C–O, and Ru–N Distances

Ru(1)–C(11)	1.860 (6)	C(11)–O(11)	1.155 (8)
Ru(1)–C(12)	1.880 (7)	C(12)–O(12)	1.142 (8)
Ru(2)–C(21)	1.905 (7)	C(21)–O(21)	1.144 (9)
Ru(2)–C(22)	1.974 (5)	C(22)–O(22)	1.128 (6)
Ru(2)–C(23)	1.898 (7)	C(23)–O(23)	1.136 (9)
Ru(3)–C(31)	1.896 (8)	C(31)–O(31)	1.145 (11)
Ru(3)–C(32)	1.939 (8)	C(32)–O(32)	1.125 (11)
Ru(3)–C(33)	1.930 (8)	C(33)–O(33)	1.133 (10)
Ru(3)–C(34)	1.936 (7)	C(34)–O(34)	1.143 (8)
Ru(1)–N(1)	2.250 (5)		

(C) Distances within $CNMe_2$ Ligand

N(2)–C(6)	1.304 (7)	N(2)–C(8)	1.486 (8)
N(2)–C(7)	1.463 (10)		

(D) Distances within py Ligand

N(1)–C(1)	1.342 (9)	C(3)–C(4)	1.344 (11)
C(1)–C(2)	1.399 (11)	C(4)–C(5)	1.382 (10)
C(2)–C(3)	1.351 (15)	C(5)–N(1)	1.351 (9)

Ru(3) bond being lengthened both relative to the Ru(1)–Ru(2) bond in the present molecule (2.885 (1) Å as opposed to 2.844 (1) Å) and to nonbridged Ru–Ru bonds in related (μ-H)Ru_3(μ-CNR_2)$(CO)_9$L species.

The μ-hydride ligand was less accurately located in this molecule; pertinent data are Ru(1)–H = 1.66 (10) Å, Ru(3)–H = 2.16 (11) Å, and ∠Ru(1)–H–Ru(2) = 93 (5)°.

Discussion

Two structures have been identified for clusters of the composition M_3L_{12}, where L is an η^1-coordinated ligand. The structure exemplified by $M_3(CO)_{12}$, M = Ru[13] or Os,[14] contains only terminally bound ligands and may be described as an anticuboctahedral packing of the 12 ligands around the metal triangle. On the other hand, the structure of $Fe_3(CO)_{12}$ in the solid state[15] contains two semibridging CO ligands along one Fe–Fe vector and may be described in terms of an icosahedral arrangement of the ligands around the Fe_3 triangle. Johnson has rationalized the structures adopted by various binary metal carbonyls and the fluxional exchange of CO ligands in terms of these two packing arrangements.[16]

If two of the 12 ligands prefer to adopt a bridged bonding mode, then the structure adopted will be of the icosahedral type, regardless of the identity of the metal.

(13) (a) Churchill, M. R.; Hollander, F. J.; Hutchinson, J. P. *Inorg. Chem.* **1977**, *16*, 2655. (b) Mason, R.; Rae, A. I. M. *J. Chem. Soc. A* **1968**, 778.

(14) Churchill, M. R.; DeBoer, B. G. *Inorg. Chem.* **1977**, *16*, 878.

(15) Cotton, F. A.; Troup, J. M. *J. Am. Chem. Soc.* **1974**, *96*, 4155 and references therein.

(16) (a) Johnson, B. F. G. *J. Chem. Soc., Chem. Commun.* **1976**, 211. (b) Benfield, R. E.; Johnson, B. F. G. *J. Chem. Soc., Dalton Trans.* **1980**, 1743.

Table V. Selected Interatomic Angles (deg) for $(\mu\text{-H})Ru_3(\mu\text{-CNMe}_2)(CO)_9(py)$

(A) Ru–Ru–Ru, Ru–C–Ru, and Ru–H–Ru Angles

Ru(2)–Ru(1)–Ru(3)	60.4 (-)	Ru(1)–C(6)–Ru(2)	88.2 (2)
Ru(1)–Ru(2)–Ru(3)	60.8 (-)	Ru(1)–H–Ru(2)	103 (4)
Ru(1)–Ru(3)–Ru(2)	58.9 (-)		

(B) Angles within μ-$CNMe_2$ Fragment

Ru(1)–C(6)–N(2)	135.8 (3)	C(6)–N(2)–C(7)	123.7 (5)
Ru(2)–C(6)–N(2)	135.7 (4)	C(6)–N(2)–C(8)	123.7 (6)
C(7)–N(2)–C(8)	112.5 (6)		

(C) Ru–Ru–Ligand Angles

Ru(2)–Ru(1)–N(1)	117.2 (1)	Ru(3)–Ru(1)–N(1)	96.9 (1)
Ru(2)–Ru(1)–H	38.4 (24)	Ru(2)–Ru(1)–C(6)	46.9 (1)
Ru(1)–Ru(2)–H	38.6 (21)	Ru(1)–Ru(2)–C(6)	44.9 (2)
Ru(3)–Ru(1)–H	81.5 (24)	Ru(3)–Ru(1)–C(6)	77.6 (2)
Ru(3)–Ru(2)–H	82.0 (25)	Ru(3)–Ru(2)–C(6)	76.9 (2)
Ru(2)–Ru(1)–C(11)	136.1 (2)	Ru(1)–Ru(3)–C(31)	98.2 (2)
Ru(2)–Ru(1)–C(12)	112.5 (2)	Ru(1)–Ru(3)–C(32)	87.8 (2)
Ru(3)–Ru(1)–C(11)	87.1 (2)	Ru(1)–Ru(3)–C(33)	158.5 (2)
Ru(3)–Ru(1)–C(12)	171.0 (2)	Ru(1)–Ru(3)–C(34)	80.4 (2)
Ru(1)–Ru(2)–C(21)	133.7 (2)	Ru(2)–Ru(3)–C(31)	157.1 (2)
Ru(1)–Ru(2)–C(22)	118.0 (2)	Ru(2)–Ru(3)–C(32)	87.3 (2)
Ru(1)–Ru(2)–C(23)	110.6 (2)	Ru(2)–Ru(3)–C(33)	99.8 (2)
Ru(3)–Ru(2)–C(21)	86.9 (2)	Ru(2)–Ru(3)–C(34)	81.1 (2)
Ru(3)–Ru(2)–C(22)	93.6 (2)	Ru(3)–Ru(1)–N(1)	96.9 (1)
Ru(3)–Ru(2)–C(23)	170.1 (1)	Ru(2)–Ru(1)–N(1)	117.2 (1)

(D) H–Ru–C and H–Ru–N Angles

H–Ru(1)–C(11)	168.1 (24)	H–Ru(2)–C(21)	168.8 (25)
H–Ru(1)–C(12)	95.8 (24)	H–Ru(2)–C(22)	86.5 (19)
H–Ru(1)–C(6)	79.8 (23)	H–Ru(2)–C(23)	93.6 (25)
H–Ru(1)–N(1)	84.4 (23)	H–Ru(2)–C(6)	78.1 (19)

(E) C–Ru–C and C–Ru–N Angles

C(11)–Ru(1)–C(12)	96.0 (3)	C(21)–Ru(2)–C(22)	94.5 (2)
C(11)–Ru(1)–N(1)	93.8 (3)	C(21)–Ru(2)–C(23)	97.4 (3)
C(12)–Ru(1)–N(1)	91.3 (2)	C(21)–Ru(2)–C(6)	99.2 (2)
C(6)–Ru(1)–C(11)	101.0 (3)	C(22)–Ru(2)–C(23)	94.9 (2)
C(6)–Ru(1)–C(12)	93.5 (3)	C(22)–Ru(2)–C(6)	162.8 (2)
C(6)–Ru(1)–N(1)	163.9 (2)	C(23)–Ru(2)–C(6)	93.6 (2)
C(31)–Ru(3)–C(32)	93.6 (3)	C(32)–Ru(3)–C(33)	93.9 (3)
C(31)–Ru(3)–C(33)	103.0 (3)	C(32)–Ru(3)–C(34)	166.6 (3)
C(31)–Ru(3)–C(34)	94.4 (3)	C(33)–Ru(3)–C(34)	94.8 (3)

(F) Ru–C–O Angles

Ru(1)–C(11)–O(11)	178.1 (7)	Ru(3)–C(31)–O(31)	179.2 (6)
Ru(1)–C(12)–O(12)	176.4 (6)	Ru(3)–C(32)–O(32)	177.6 (7)
Ru(2)–C(21)–O(21)	178.9 (6)	Ru(3)–C(33)–O(33)	178.5 (7)
Ru(2)–C(22)–O(22)	177.9 (6)	Ru(3)–C(34)–O(34)	177.4 (6)
Ru(2)–C(23)–O(23)	179.0 (5)		

(G) Angles Involving py Ligand

Ru(1)–N(1)–C(1)	123.5 (4)	C(1)–C(2)–C(3)	120.3 (8)
Ru(1)–N(1)–C(5)	119.4 (4)	C(2)–C(3)–C(4)	118.4 (8)
C(1)–N(1)–C(5)	116.8 (5)	C(3)–C(4)–C(5)	120.4 (8)
N(1)–C(1)–C(2)	121.7 (8)	C(4)–C(5)–N(1)	122.4 (6)

Thus, there are a large number of compounds of the general formula $M_3(\mu\text{-X})(\mu\text{-Y})(CO)_{10}$, where M = Fe, Ru, or Os and X and Y are halogens, hydrogen, ER (E = group 16[36] atom), ER_2 (E = group 15[36] atom), or some combination of these.

Although several synthetic or mechanistic studies of ligand substitution on these clusters have been reported,[17-29] little has been established regarding the substitutional isomerism in this class. For the vast majority of monosubstituted products $M_3(\mu\text{-X})(\mu\text{-Y})(CO)_9L$ which

Table VI. Interatomic Distances (Å), with Esd's, for $(\mu\text{-H})Ru_3(\mu\text{-CNBz}_2)(CO)_9(PPh_3)$

(A) Ru–Ru and Ru–(Bridging Ligand) Distances

Ru(1)–Ru(2)	2.844 (1)	Ru(1)–C(1)	2.052 (10)
Ru(1)–Ru(3)	2.792 (1)	Ru(3)–C(1)	2.041 (11)
Ru(2)–Ru(3)	2.885 (1)	Ru(1)–H	1.66 (10)
		Ru(3)–H	2.16 (11)

(B) Ru–CO, C–O, and Ru–P Distances

Ru(1)–C(11)	1.865 (13)	C(11)–O(11)	1.164 (16)
Ru(1)–C(12)	1.938 (12)	C(12)–O(12)	1.107 (15)
Ru(1)–C(13)	1.984 (11)	C(13)–O(13)	1.087 (14)
Ru(2)–C(21)	1.866 (12)	C(21)–O(21)	1.162 (15)
Ru(2)–C(22)	1.876 (11)	C(22)–O(22)	1.171 (14)
Ru(2)–C(23)	1.904 (12)	C(23)–O(23)	1.164 (15)
Ru(3)–C(31)	1.852 (12)	C(31)–O(31)	1.167 (15)
Ru(3)–C(32)	1.879 (11)	C(32)–O(32)	1.150 (14)
Ru(3)–C(33)	1.931 (12)	C(33)–O(33)	1.155 (15)
Ru(2)–P	2.384 (2)		

(C) Carbon–Nitrogen Distances within $CNBz_2$ Ligand

N(1)–C(1)	1.288 (14)	N(1)–C(3)	1.505 (13)
N(1)–C(2)	1.482 (13)		

(D) Carbon–Carbon Distances within $CNBz_2$ Ligand

C(2)–C(4)	1.504 (15)	C(3)–C(5)	1.533 (17)
C(4)–C(41)	1.349 (18)	C(5)–C(51)	1.392 (16)
C(4)–C(45)	1.382 (18)	C(5)–C(55)	1.353 (18)
C(41)–C(42)	1.396 (24)	C(51)–C(52)	1.381 (20)
C(42)–C(43)	1.361 (28)	C(52)–C(53)	1.309 (21)
C(43)–C(44)	1.327 (29)	C(53)–C(54)	1.338 (23)
C(44)–C(45)	1.384 (26)	C(54)–C(55)	1.419 (22)

(E) Phosphorus–Carbon Distances within PPh_3 Ligand

P–C(61)	1.833 (10)	P–C(81)	1.852 (10)
P–C(71)	1.843 (11)		

(F) Carbon–Carbon Distances within PPh_3 Ligand

C(61)–C(62)	1.405 (15)	C(71)–C(72)	1.397 (17)
C(62)–C(63)	1.389 (18)	C(72)–C(73)	1.384 (19)
C(63)–C(64)	1.369 (20)	C(73)–C(74)	1.334 (18)
C(64)–C(65)	1.435 (20)	C(74)–C(75)	1.356 (18)
C(65)–C(66)	1.384 (19)	C(75)–C(76)	1.397 (17)
C(66)–C(61)	1.369 (15)	C(76)–C(71)	1.370 (16)
C(81)–C(82)	1.389 (15)	C(84)–C(85)	1.322 (21)
C(82)–C(83)	1.406 (17)	C(85)–C(86)	1.410 (19)
C(83)–C(84)	1.332 (21)	C(86)–C(81)	1.372 (17)

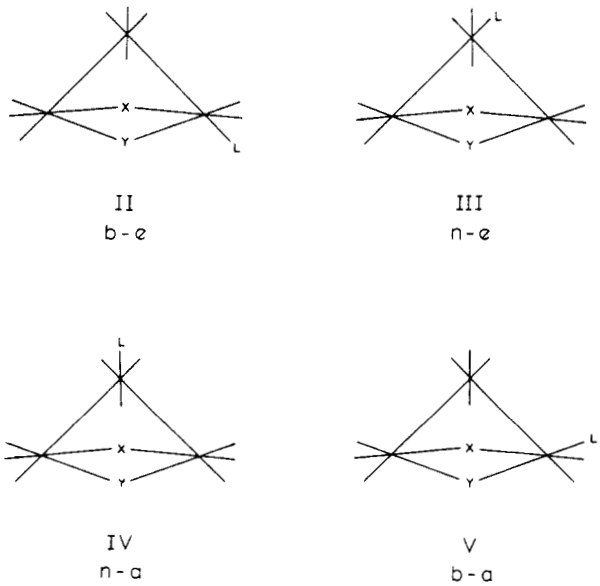

Figure 5. Schematic diagram of bridged-equatorial (b-e), II, nonbridged-equatorial (n-e), III, nonbridged-axial (n-a), IV, and bridged-axial (b-a), V, isomers, of $M_3(\mu\text{-X})(\mu\text{-Y})(CO)_9L$.

(17) (a) Norton, J. R.; Collman, J. P. *Inorg. Chem.* **1973**, *12*, 476. (b) Grant, S. M.; Manning, A. R. *Inorg. Chim. Acta* **1978**, *31*, 41. (c) Shojaie, A.; Atwood, J. D. *Organometallics* **1985**, *4*, 187. (d) Deeming, A. J.; Johnson, B. F. G.; Lewis, J. *J. Chem. Soc. A* **1970**, 897. (e) Deeming, A. J.; Johnson, B. F. G.; Lewis, J. *J. Chem. Soc. A* **1970**, 2517.

(18) Deeming, A. J.; Manning, P. J.; Rothwell, I. P.; Hursthouse, M. B.; Walker, N. P. C. *J. Chem. Soc., Dalton Trans.* **1984**, 2039.

(19) Adams, R. D.; Katahira, D. A.; Yang, L.-W. *J. Organomet. Chem.* **1981**, *219*, 241.

(20) Adams, R. D.; Katahira, D. A.; Yang, L.-W. *J. Organomet. Chem.* **1981**, *219*, 85.

(21) Johnson, B. F. G.; Lewis, J.; Raithby, P. R.; Zuccaro, C. *J. Chem. Soc., Chem. Commun.* **1979**, 916.

(22) Adams, R. D.; Golembeski, N. M. *Inorg. Chem.* **1979**, *18*, 1909.

Table VII. Selected Interatomic Angles (deg) for $(\mu\text{-}H)Ru_3(\mu\text{-}CNBz_2)(CO)_9(PPh_3)$

(A) Ru–Ru–Ru, Ru–C–Ru, and Ru–H–Ru Angles

Ru(2)–Ru(1)–Ru(3)	61.57 (3)	Ru(1)–C(1)–Ru(3)	86.0 (4)
Ru(1)–Ru(2)–Ru(3)	58.32 (3)	Ru(1)–H–Ru(3)	93 (5)
Ru(1)–Ru(3)–Ru(2)	60.11 (3)		

(B) Ru–C–N, C–N–C, and N–C–C Angles within μ-$CNBz_2$ Fragment

Ru(1)–C(1)–N(1)	136.6 (8)	C(1)–N(1)–C(2)	122.6 (9)
Ru(3)–C(1)–N(1)	136.2 (8)	C(1)–N(2)–C(3)	122.8 (9)
C(2)–N(1)–C(3)	114.0 (8)	N(1)–C(2)–C(4)	113.9 (9)
		N(1)–C(3)–C(5)	111.5 (9)

(C) Ru–Ru–Ligand Angles

Ru(2)–Ru(1)–H	105 (4)	Ru(2)–Ru(1)–C(1)	78.3 (3)
Ru(3)–Ru(1)–H	51 (4)	Ru(3)–Ru(1)–C(1)	46.8 (3)
Ru(1)–Ru(3)–H	36 (3)	Ru(1)–Ru(3)–C(1)	47.1 (3)
Ru(2)–Ru(3)–H	91 (3)	Ru(2)–Ru(3)–C(1)	77.4 (3)
Ru(2)–Ru(1)–C(11)	87.1 (4)	Ru(1)–Ru(2)–C(21)	94.0 (4)
Ru(3)–Ru(1)–C(11)	135.3 (4)	Ru(3)–Ru(2)–C(21)	152.2 (4)
Ru(2)–Ru(1)–C(12)	175.8 (3)	Ru(1)–Ru(2)–C(22)	85.2 (3)
Ru(3)–Ru(1)–C(12)	114.3 (3)	Ru(3)–Ru(2)–C(22)	82.6 (3)
Ru(2)–Ru(1)–C(13)	90.4 (3)	Ru(1)–Ru(2)–C(23)	86.8 (4)
Ru(3)–Ru(1)–C(13)	113.5 (3)	Ru(3)–Ru(2)–C(23)	90.5 (4)
Ru(1)–Ru(3)–C(31)	112.8 (4)	Ru(1)–Ru(2)–P	169.98 (7)
Ru(2)–Ru(3)–C(31)	170.3 (4)	Ru(3)–Ru(2)–P	111.67 (7)
Ru(1)–Ru(3)–C(32)	132.5 (3)	Ru(1)–Ru(3)–C(33)	113.7 (4)
Ru(2)–Ru(3)–C(32)	82.9 (3)	Ru(2)–Ru(3)–C(33)	95.5 (4)

(D) H–Ru–C Angles

H–Ru(1)–C(1)	78 (4)	H–Ru(3)–C(1)	68 (3)
H–Ru(1)–C(11)	166 (4)	H–Ru(3)–C(31)	84 (3)
H–Ru(1)–C(12)	71 (4)	H–Ru(3)–C(32)	167 (3)
H–Ru(1)–C(13)	90 (4)	H–Ru(3)–C(33)	95 (3)

(E) C–Ru–C and P–Ru–C Angles

C(1)–Ru(1)–C(11)	99.0 (5)	C(21)–Ru(2)–C(22)	94.6 (5)
C(1)–Ru(1)–C(12)	98.4 (5)	C(21)–Ru(2)–C(23)	89.1 (5)
C(1)–Ru(1)–C(13)	160.2 (4)	C(22)–Ru(2)–C(23)	171.4 (5)
C(11)–Ru(1)–C(12)	96.0 (5)	C(1)–Ru(3)–C(31)	92.9 (5)
C(11)–Ru(1)–C(13)	96.6 (5)	C(1)–Ru(3)–C(32)	99.5 (5)
C(12)–Ru(1)–C(13)	92.0 (5)	C(1)–Ru(3)–C(33)	160.6 (5)
P–Ru(2)–C(21)	96.1 (4)	C(31)–Ru(3)–C(32)	99.4 (5)
P–Ru(2)–C(22)	94.2 (3)	C(31)–Ru(3)–C(33)	93.6 (5)
P–Ru(2)–C(23)	93.1 (4)	C(32)–Ru(3)–C(33)	97.5 (5)

(F) Ru–C–O Angles

Ru(1)–C(11)–O(11)	178.4 (10)	Ru(2)–C(23)–O(23)	174.4 (10)
Ru(1)–C(12)–O(12)	177.1 (11)	Ru(3)–C(31)–O(31)	175.4 (10)
Ru(1)–C(13)–O(13)	175.1 (10)	Ru(3)–C(32)–O(32)	177.4 (10)
Ru(2)–C(21)–O(21)	176.9 (11)	Ru(3)–C(33)–O(33)	176.4 (11)
Ru(2)–C(22)–O(22)	178.4 (10)		

(G) Ru–P–C and C–P–C Angles

Ru(2)–P–C(61)	111.4 (3)	C(61)–P–C(71)	104.0 (5)
Ru(2)–P–C(71)	116.3 (4)	C(61)–P–C(81)	103.3 (5)
Ru(2)–P–C(81)	121.2 (3)	C(71)–P–C(81)	98.5 (5)

(H) C–C–C Angles in Bz Groups

C(2)–C(4)–C(41)	121.9 (10)	C(3)–C(5)–C(51)	119.4 (10)
C(2)–C(4)–C(45)	117.4 (10)	C(3)–C(5)–C(55)	121.4 (11)
C(45)–C(4)–C(41)	120.6 (12)	C(55)–C(5)–C(51)	119.2 (11)
C(4)–C(41)–C(42)	120.8 (13)	C(5)–C(51)–C(52)	120.1 (12)
C(41)–C(42)–C(43)	118.8 (17)	C(51)–C(52)–C(53)	119.9 (13)
C(42)–C(43)–C(44)	119.4 (18)	C(52)–C(53)–C(54)	122.2 (15)
C(43)–C(44)–C(45)	123.8 (18)	C(53)–C(54)–C(55)	119.8 (15)
C(44)–C(45)–C(4)	116.4 (14)	C(54)–C(55)–C(5)	118.7 (13)

(I) C–C–C and P–C–C Angles in PPh_3 Group

C(66)–C(61)–C(62)	118.7 (10)	C(86)–C(81)–C(82)	116.7 (10)
C(61)–C(62)–C(63)	120.9 (11)	C(81)–C(82)–C(83)	120.9 (10)
C(62)–C(63)–C(64)	120.5 (12)	C(82)–C(83)–C(84)	118.5 (12)
C(63)–C(64)–C(65)	118.8 (13)	C(83)–C(84)–C(85)	124.0 (14)
C(64)–C(65)–C(66)	119.5 (13)	C(84)–C(85)–C(86)	117.8 (13)
C(65)–C(66)–C(61)	121.5 (11)	C(85)–C(86)–C(81)	122.0 (12)
C(76)–C(71)–C(72)	116.7 (10)	P–C(61)–C(62)	118.8 (8)
C(71)–C(72)–C(73)	120.7 (12)	P–C(61)–C(66)	122.3 (8)
C(72)–C(73)–C(74)	120.2 (12)	P–C(71)–C(76)	123.5 (9)
C(73)–C(74)–C(75)	121.8 (12)	P–C(71)–C(72)	119.8 (9)
C(74)–C(75)–C(76)	118.2 (12)	P–C(81)–C(86)	117.2 (8)
C(75)–C(76)–C(71)	122.3 (11)	P–C(81)–C(82)	126.0 (8)

have been characterized by spectroscopic or crystallographic methods, L is coordinated in an equatorial position on one of the bridged metal atoms (Figure 5, structure II, bridged-equatorial (b-e) isomer, e.g., $(\mu\text{-}H)Os_3(\mu\text{-}OH)(CO)_9(PPh_3)$,[18] *syn*-$(\mu\text{-}H)Os_3(\mu\text{-}NCHCF_3)(CO)_9(PMe_2Ph)$,[19] *anti*-$(\mu\text{-}H)Os_3(\mu\text{-}NCHCF_3)(CO)_9(PMe_2Ph)$,[20] $Os_3(\mu\text{-}NO)_2(CO)_9(NMe_3)$,[21] $(\mu\text{-}H)_2Os_3(CO)_9(CNCMe_3)$,[22] or one isomer of $Fe_3(\mu\text{-}CO)_2(CO)_9(PPh_3)$[23]). Very few examples are known in which L is coordinated to the nonbridged metal atom in either equatorial (Figure 5, structure III, nonbridged-equatorial (n-e) isomer, e.g., one isomer of $Fe_3(\mu\text{-}CO)_2(CO)_9(PPh_3)$,[23] $RuFe_2(\mu\text{-}CO)_2(CO)_9(PPh_3)$,[24] or $(\mu\text{-}H)Os_3(\mu\text{-}SMe)(CO)_9(C_2H_4)$[25]) or axial (Figure 5, structure IV, nonbridged -axial (n-a) isomer, e.g., $Fe_3(\mu\text{-}CO)_2(CO)_9(CNCMe_3)$[26] or $(\mu\text{-}H)Os_3(\mu\text{-}COMe)(CO)_9(CNCMe_3)$[27]) positions. The trisubstituted clusters $(\mu\text{-}H)Ru_3(\mu\text{-}NO)(CO)_7(P(OMe)_3)_3$[28] and $Fe_3(\mu\text{-}CO)_2(CO)_7(PMe_2Ph)_3$[29] contain both b-e and n-e coordinated phosphorus donor ligands, but spectroscopic data suggest that the mono- and disubstituted derivatives contain only b-e ligands. Prior to this work there were no known examples of bridged-axial (b-a) isomers (Figure 5, structure V). In very few instances were the substitution products known to be thermodynamically rather than kinetically determined and only for $Fe_3(\mu\text{-}CO)_2(CO)_9(PPh_3)$[23] were two isomers having the same ligand composition available. Thus, it has not been possible to make conclusions regarding the steric and electronic factors responsible for the determination of the structure adopted.

Recently one of us reported that the substitution products $(\mu\text{-}H)Ru_3(\mu\text{-}CX)(CO)_9L$ (X = OMe or NR_2; L = PR_3, $AsPh_3$, or $SbPh_3$) exist in solution as equilibrium mixtures of two isomers.[7] One of these was characterized as the b-e isomer by spectroscopic methods. The other isomer is shown in this paper to be the n-e isomer, which is thermodynamically most stable for $(\mu\text{-}H)Ru_3(\mu\text{-}CNBz_2)(CO)_9(PPh_3)$. We have also shown here that $(\mu\text{-}H)Ru_3(\mu\text{-}CNMe_2)(CO)_9(py)$ exists in the crystalline state as the previously unknown b-a isomer. Spectroscopic data indicate that these two clusters exist in the same form in solution. A fourth isomeric form is adopted by the closely related $(\mu\text{-}H)Os_3(\mu\text{-}COMe)(CO)_9(CNCMe_3)$, which exists in solution and in the solid state of the n-a isomer.[27]

The isomerism of $(\mu\text{-}H)Ru_3(\mu\text{-}CX)(CO)_9L$ offers a unique opportunity to examine the steric and electronic properties which determine the thermodynamic stabilities of the various structures. We have previously established that the kinetic product from ligand substitution by phosphines, arsines, or stibines on $(\mu\text{-}H)Ru_3(\mu\text{-}CX)(CO)_{10}$ is the n-e isomer and that a relatively rapid intramolecular rearrangement converts this product to the equilibrium mixture containing the b-e form.[7] Thus, the relative ratios of these isomer are determined by thermodynamics. The equilibrium amounts of n-e and b-e isomers of $(\mu\text{-}H)Ru_3(\mu\text{-}CX)(CO)_9L$ vary with the identities of X and of L. For L = PPh_3, the n-e:b-e ratio increases in the order: X = O^- (0:1) $\approx$ OMe (0:1) < NMe_2 (0.12:0.87) < NBz_2 (1:0). For X = NMe_2 the n-e:b-e ratio increases in the order: L = PPh_3 < $AsPh_3$ < $SbPh_3$ and L = PPh_3 $\lesssim$ $P(C_6H_{11})_3$ <

(23) Dahm, D. J.; Jacobson, R. A. *J. Am. Chem. Soc.* **1968**, *90*, 5106.
(24) Venäläinen, T.; Pakkanen, T. *J. Organomet. Chem.* **1984**, *266*, 269.
(25) Johnson, B. F. G.; Lewis, J.; Pippard, D.; Raithby, P. R. *J. Chem. Soc., Chem. Commun.* **1978**, 551.
(26) Bruce, M. I.; Nicholson, B. K.; White, A. H. *J. Organomet. Chem.* **1982**, *240*, C33.
(27) Gavens, P. D.; Mays, M. J. *J. Organomet. Chem.* **1978**, *162*, 389.
(28) Johnson, B. F. G.; Raithby, P. R.; Zuccaro, C. *J. Chem. Soc., Dalton Trans.* **1980**, 99.
(29) Raper, G.; McDonald, W. S. *J. Chem. Soc. A* **1971**, 3430.

$P(OPh)_3 < PBu_3$. These data suggest that both steric and electronic factors influence the value of the equilibrium constant but that for a given L the predominant influence of X is due to steric effects. As the size of X increases, the relative stability of the b-e isomer decreases. With the structures of $(\mu\text{-H})Ru_3(\mu\text{-CX})(CO)_{10}$ (X = OMe[1,4] and NMe_2[2]), $(\mu\text{-H})Ru_3(\mu\text{-CNMe}_2)(CO)_9(py)$, and $(\mu\text{-H})Ru_3(\mu\text{-CNBz}_2)(CO)_9(PPh_3)$ in hand and with the information provided by the n-e:b-e ratios for $(\mu\text{-H})Ru_3(\mu\text{-CX})(CO)_9L$, some generalizations can be made regarding the factors which determine the isomeric form adopted by these complexes.

The packing of the 12 ligands around $(\mu\text{-H})Ru_3(\mu\text{-CX})(CO)_9L$ (X = O^-, L = CO;[30] X = OMe, L = CO;[1,4] X = NMe_2, L = CO;[2] X = NMe_2, L = py; X = NBz_2, L = PPh_3) may be described as icosahedral, with relatively minor differences in the structure for various X and L substituents. Comparisons of the structures of $(\mu\text{-H})Ru_3(\mu\text{-COMe})(CO)_{10}$, $(\mu\text{-H})Ru_3(\mu\text{-CNMe}_2)(CO)_{10}$, $(\mu\text{-H})Ru_3(\mu\text{-CNMe}_2)(CO)_9(py)$, and $(\mu\text{-H})Ru_3(\mu\text{-CNBz}_2)(CO)_9(PPh_3)$ show no significant variations in either the average Ru–Ru bond distance (2.825, 2.819, 2.832, and 2.840 Å, respectively) or in the average Ru–CO bond distances (1.931, 1.922, 1.913, and 1.899 Å, respectively). There is no evidence to suggest that the radius of the ligand shell or of the Ru_3 triangle is significantly influenced by replacement of a CO ligand by py or by PPh_3.

All the Ru atoms in these structures may be regarded as having octahedral coordination geometries. For example, the unique Ru atom of $(\mu\text{-H})Ru_3(\mu\text{-CNMe}_2)(CO)_{10}$[2] is coordinated to four CO ligands (one cis and one trans pair) and two Ru atoms, while each bridged Ru atom is coordinated to three *fac* CO ligands, one Ru atom, the bridging hydride, and the bridging $CNMe_2$ ligand. There is no structural evidence for a direct Ru–Ru interaction along the bridged edge; the bonding between the bridged metals may be considered to occur through a multicenter interaction involving the bridging groups.[31] Thus, the coordination number for each Ru atom is six. Steric requirements for ligands occupying each site will be determined by the four cis ligands and to a smaller extent by the ligands on adjacent metal atoms. Angles between the b-e CO and the four cis ligands are 94.7° (CO trans to H), 97.7° (CO trans to $CNMe_2$), 97.8 ($CNMe_2$), and 90.7° (H) (average angle 95°), while those between the n-e CO ligand and the four cis ligands are 91.5° (axial CO), 93.7° (axial CO), 104.3° (equatorial CO), and 102.9° (Ru) (average angle 98°).

On the basis of π-bonding arguments, the most stable isomers would be expected to contain σ-donor ligands trans to good π-acceptor ligands. It has been noted that the μ-COMe and μ-CNR_2 ligands are very good π-acceptors, so much so that they exert a stronger trans influence than CO. Evidence for this comes from the very long Ru–CO distances trans to the μ-CX ligand in the structures of $(\mu\text{-H})Ru_3(\mu\text{-CX})(CO)_{10}$ (X = O^-,[30] OMe,[1,4] and NMe_2[2]). The shorter Ru-$CNMe_2$ distance trans to py (1.977 Å, cf. 2.047 Å for the Ru-$CNMe_2$ distance trans to CO) in the structure of $(\mu\text{-H})Ru_3(\mu\text{-CNMe}_2)(CO)_9(py)$ is indicative of enhanced π-back-bonding to $CNMe_2$ when it is trans to a good σ-donor. Thus, strictly on the basis of maximized π-back-bonding, one would expect the thermodynamically most stable isomer of $(\mu\text{-H})Ru_3(\mu\text{-CX})(CO)_9L$ (X = O^-, OMe, or NR_2; L = PR_3 or py) to be the b-a form. This is the case for $(\mu\text{-H})Ru_3(\mu\text{-CNMe}_2)(CO)_9(py)$, but all phosphine derivatives are either b-e or n-e isomers in the ground state. This may be readily explained on steric grounds. The small py ligand may occupy the b-a position with little distortion (average angle between the py–Ru vector and the four cis Ru–ligand vectors, 91.6°; average angle between the Ru(2)–C(23) vector and the four cis Ru–ligand vectors for $(\mu\text{-H})Ru_3(\mu\text{-CNMe}_2)(CO)_{10}$, 92.4°) but the phosphines are too large to occupy axial positions due to unfavorable interactions with axial carbonyls on the adjacent metal atoms. This trend is also found for M_3L_{12} structures having anticuboctahedral ligand packings; phosphines and other large ligands coordinate equatorially,[32] but small ligands such as isocyanides, nitriles, and pyridines coordinate trans to CO ligands in axial positions.[32c,33]

There still remains the problem of rationalizing the relative stabilities of b-e vs. n-e and b-a vs. n-a isomers. While the bridged and nonbridged metal atoms obviously differ in both steric and electronic characteristics, it is difficult to make a judgement as to which site would be prefered by a given ligand on either basis. Not enough examples of b-a and n-a complexes are available to allow comparisons of these forms. A later paper will address variation in the relative stabilities of b-e and n-e forms upon changes in the electronic properties of L.[34] Here we will focus only upon the differences in the steric requirements of b-e and n-e coordination sites.

Three types of nonbonded contacts will be important—those between L and the four cis ligands on the same metal, those between L and the carbonyls on the adjacent metal, and those between L and the alkyl groups on the methylidyne substituent. If only nonbonded interactions between L and the four ligands cis to L are considered, then the n-e coordination site is somewhat less congested than the b-e site (cf. average angles to cis ligands for $(\mu\text{-H})Ru_3(\mu\text{-CNMe}_2)(CO)_{10}$, n-e 98°, b-e 95°). However, the substituents on phosphorus will also interact with carbonyl ligands on the adjacent metal site. Since the packing of the twelve ligands is icosahedral, each ligand will have five neighbors which must be considered. When L is in the b-e position, the five adjacent ligands will be the four cis ligands coordinated to the same metal (two b-a carbonyls, μ-H, and μ-CX), already considered, and the b-e carbonyl on the adjacent metal atom; when L is in the n-e position, the five neighbors will be the three cis carbonyls on the same metal, already considered, and the two b-a carbonyls on the adjacent metal atom. Thus, at the second level, one more non-bonded interaction is involved when L is n-e than when L is b-e. Furthermore, the substituents on phosphorus can be more easily oriented to minimize nonbonded contacts with the CO ligand(s) on the adjacent metal atom when the phosphine is in the b-e position. Because of these "secondary" interactions, the b-e form is more favorable than the n-e form in terms of minimization of nonbonded repulsions.

Structural evidence for this comes from the changes in interligand angles around the metal atom upon substitution of a CO by a phosphine. Phosphine substitution in the b-e position causes only minor changes in these angles. For example, the average angle between the P–Fe vector

(30) Johnson, B. F. G.; Lewis, J.; Raithby, P. R.; Süss, G. *J. Chem. Soc., Dalton Trans.* **1979**, 1356.
(31) Chesky, P. T.; Hall, M. B. *Inorg. Chem.* **1983**, *22*, 3327.
(32) (a) Johnson, B. F. G.; Lewis, J.; Reichert, B. E.; Schorpp, K. T. *J. Chem. Soc., Dalton Trans.* **1976**, 1403. (b) Forbes, E. J.; Goodhand, N.; Jones, D. L.; Hamor, T. A. *J. Organomet. Chem.* **1979**, *182*, 143. (c) Keister, J. B.; Shapley, J. R. *Inorg. Chem.* **1982**, *21*, 3304.
(33) (a) Mays, M. J.; Gavens, P. D. *J. Chem. Soc., Dalton Trans.* **1980**, 911. (b) Johnson, B. F. G.; Lewis, J.; Pippard, D. A. *J. Chem. Soc., Dalton Trans.* **1981**, 407. (c) Bruce, M. I.; Schultz, D.; Wallis, R. C.; Redhouse, A. D. *J. Organomet. Chem.* **1979**, *169*, C15.
(34) Shaffer, M. R.; Keister, J. B., submitted for publication in *Organometallics*.

and the four cis Fe–CO vectors in the structure of b-e-$Fe_3(\mu\text{-}CO)_2(CO)_9(PPh_3)$ is 94°, and the average angle between a b-e-Fe–CO and the four cis Fe–CO vectors in n-e-$Fe_3(\mu\text{-}CO)_2(CO)_9(PPh_3)$ is also 94°.[23] On the other hand, phosphine substitution in an n-e position significantly increases the n-e ligand–metal–metal angle. For example, for (μ-H)$Ru_3(\mu\text{-}CNMe_2)(CO)_{10}$ the n-e CO–Ru–Ru angle is 100°, but for (μ-H)$Ru_3(\mu\text{-}CNBz_2)(CO)_9(PPh_3)$ the n-e P–Ru–Ru angle is 112°. This increase in the n-e ligand–metal–metal angle has been noted in all structures containing n-e phosphine ligands.

As the methylidyne substituent becomes larger, nonbonded interactions between the b-e ligand and the methylidyne will increase, while those involving the n-e ligand will not. This explains the change in the n-e:b-e ratio in the series (μ-H)$Ru_3(\mu\text{-}CX)(CO)_9(PPh_3)$: X = O^- ≈ OMe < NMe_2 < NBz_2. When X = NMe_2, the b-e isomer is 1.2 kcal more stable than the n-e isomer.[7] For X = NBz_2, the benzyl groups adopt a conformation such that a phenyl ring is located over the b-e position (Figure 3), thus increasing nonbonded repulsions with the b-e ligand to the extent that only the n-e isomer is observed.

The magnitude of the steric repulsions between the alkyl groups on X and L has been measured directly in the case of (μ-H)$Os_3(\mu\text{-}COMe)(CO)_9(PPh_3)$, which adopts the b-e structure.[35] Two rotamers differing in the relative orientation of the methyl group and the PPh_3 ligand interconvert with a free energy of activation of 16.1 kcal/mol. The anti rotamer is more stable than the syn rotamer by 0.4 kcal. Steric interactions between L and the alkyl groups of the methylidyne substituent should be even more important for the Ru analogues.

Coupling reactions of substrates on cluster surfaces require that the substrates occupy adjacent coordination sites. Thus, the reactivity for various metal clusters may be explained by the steric and electronic effects upon structural isomerism. One example pertinent to the clusters discussed in this work is the reaction between (μ-H)$Ru_3(\mu\text{-}COMe)(CO)_{10}$ and alkynes C_2R_2 to form $HRu_3(\mu_3\text{-}\eta^3\text{-}MeOCCRCR)(CO)_9$.[6] This reaction does not occur for the (dimethylamino)methylidyne analogue, and one explanation for its lack of reactivity is that the more unfavorable nonbonded interactions between the alkyne and the $CNMe_2$ ligand make the requisite cis isomer unstable.

Electronic effects will also influence the structure adopted by $M_3(\mu\text{-}X)(\mu\text{-}Y)(CO)_9L$ clusters. In the next paper in this series we will examine the influence of the ligand on the n-e to b-e isomerization.[34]

Acknowledgment. This research was supported by the National Science Foundation under Grants No. CHE-8121059 (J.B.K.) and CHE-8023448 (M.R.C.).

Registry No. (μ-H)$Ru_3(\mu\text{-}CNMe_2)(CO)_9$(Py), 97415-87-7; ($\mu$-H)$Ru_3(\mu\text{-}CNBz_2)_9(PPh_3)$, 97415-88-8.

Supplementary Material Available: Tables of observed and calculated structure factor amplitudes and anisotropic thermal parameters for both (μ-H)$Ru_3(\mu\text{-}CNMe_2)(CO)_9$(py) and ($\mu$-H)-$Ru_3(\mu\text{-}CNBz_2)(CO)_9(PPh_3)$ (46 pages). Ordering information is given on any current masthead page.

(35) Bavaro, L. M.; Keister, J. B. *J. Organomet. Chem.* **1985**, *287*, 357.

(36) In this paper the periodic group notation is in accord with recent actions by IUPAC and ACS nomenclature committees. A and B notation is eliminated because of wide confusion. Groups IA and IIA become groups 1 and 2. The d-transition elements comprise groups 3 through 12, and the p-block elements comprise groups 13 through 18. (Note that the former Roman number designation is preserved in the last digit of the new numbering: e.g., III → 3 and 13.)